Magnon Condensation into a Q Ball in ^{3}He-B

Yu. M. Bunkov[1] and G. E. Volovik[2,3]
[1]*Institute Neel, CNRS-UJF, Grenoble, France*
[2]*Low Temperature Laboratory, Helsinki University of Technology, Helsinki, Finland*
[3]*L. D. Landau Institute for Theoretical Physics, Moscow, Russia*
(Received 9 March 2007; published 29 June 2007)

The theoretical prediction of Q balls in relativistic quantum fields is realized here experimentally in superfluid ^{3}He-B. The condensed-matter analogs of relativistic Q balls are responsible for an extremely long-lived signal of magnetic induction observed in NMR at the lowest temperatures. This Q ball is another representative of a state with phase coherent precession of nuclear spins in ^{3}He-B, similar to the well-known homogeneously precessing domain, which we interpret as Bose-Einstein condensation of spin waves—magnons. At large charge Q, the effect of self-localization is observed. In the language of relativistic quantum fields it is caused by interaction between the charged and neutral fields, where the neutral field provides the potential for the charged one. In the process of self-localization the charged field modifies locally the neutral field so that the potential well is formed in which the charge Q is condensed.

DOI: 10.1103/PhysRevLett.98.265302 PACS numbers: 67.57.Fg, 05.45.Yv, 11.27.+d

A Q ball is a nontopological soliton solution in field theories containing a complex scalar field ϕ. Q balls are stabilized due to the conservation of the global $U(1)$ charge Q [1]: they exist if the energy minimum develops at nonzero ϕ at fixed Q. At the quantum level, a Q ball is formed due to a suitable attractive interaction that binds the quanta of the ϕ field into a large compact object. In some modern supersymmetry scenarios, Q balls are considered as heavy particlelike objects, with Q being the baryon and/or lepton number. For many conceivable alternatives, Q balls may contribute significantly to the dark matter and baryon content of the Universe, as described in review [2]. Stable cosmological Q balls can be searched for in existing and planned experiments [3].

The Q ball is a rather general physical object, which in principle can be formed in condensed-matter systems. In particular, Q balls were suggested in the atomic Bose-Einstein condensates [4]. Here we report the observation of Q balls in NMR experiments in superfluid ^{3}He-B, where the Q balls are formed as special states of phase coherent precession of magnetization. The role of the Q charge is played by the projection of the total spin of the system on the axis of the magnetic field, which is a rather well-conserved quantity at low temperature. At the quantum level, this Q ball is a compact object formed by magnons—quanta of the corresponding ϕ field.

Two types of coherent precession of magnetization have been observed in superfluid ^{3}He-B. The first state known as the homogeneously precessing domain (HPD) was discovered in 1984 [5]. This is the bulk state of precessing magnetization that exhibits all the properties of spin superfluidity and Bose condensation of magnons (see reviews [6,7]). These include, in particular, spin supercurrent which transports the magnetization (analog of the mass current in superfluids and electric supercurrent in superconductors), spin current Josephson effect and phase-slip processes at the critical current, and spin current vortex—a topological defect which is the analog of a quantized vortex in superfluids and of an Abrikosov vortex in superconductors.

The HPD loses stability at low temperatures (below about $0.4T_c$), which is now well understood in terms of a parametric instability of precession toward a decay into pairs of spin waves, which is known as the Suhl instability; see Ref. [8]. In its stead another type of coherent precession has been found [9]. This new state occupies only a small fraction of the volume of the sample (the signal from such a state is typically below 1% of the HPD signal). It can be independently generated in different parts of the sample, with the signal being dependent on the position in the container. Such a state lives extremely long, up to a few minutes, without external pumping [9,10]. That is why the name persistent signal (PS) is used. We shall show here that the PS has the perfect formal analogy with the Q ball.

Both the HPD and PS states can be described in terms of Bose-Einstein condensation of magnons. The complex order parameter Ψ of the magnon condensate is related to the precessing spin in the following way [6]:

$$\Psi = \sqrt{2S/\hbar}\,\sin\frac{\beta}{2}\,e^{i\omega t+i\alpha}, \qquad S_x + iS_y = S\sin\beta e^{i\omega t+i\alpha}. \tag{1}$$

Here $\mathbf{S} = (S_x, S_y, S_z = S\cos\beta)$ is the vector of spin density; β is the tipping angle of precessing magnetization; ω is the precession frequency (in the regime of continuous NMR, it is the frequency of the applied rf field and it plays the role of the chemical potential $\mu = -\omega$ for magnons); α is the phase of precession; $S = \chi H/\gamma$ is the equilibrium value of spin density in the applied magnetic field $\mathbf{H} = H\hat{\mathbf{z}}$; χ is spin susceptibility of liquid ^{3}He-B; and γ is the gyromagnetic ratio of the ^{3}He atom. The charge Q

$$Q = \int d^3r|\Psi|^2 = \int d^3r\,\frac{S - S_z}{\hbar} \tag{2}$$

is the number of magnons in the precessing state. It is a

conserved quantity if one neglects the spin-orbit interaction, which is relatively small in ^{3}He-B.

The corresponding Gross-Pitaevskii equation is ($\hbar = 1$)

$$[\omega - \omega_L(z)]\Psi = \frac{\delta F}{\delta \Psi^*}, \tag{3}$$

$$F = \int d^3r \left(\frac{|\nabla \Psi|^2}{2m_M} + F_D \right). \tag{4}$$

Here $\omega_L(z) = \gamma H(z)$ is the Larmor frequency, which slightly depends on z when the field gradient is applied; $m_M = \omega_L/2c^2$ is the magnon mass, where c is the spin-wave velocity; and F_D the spin-orbit (dipole) interaction averaged over the fast precession. This interaction is typically small so that the precession frequency $\omega \approx \omega_L$.

The connection to relativistic Q balls becomes clear if one introduces the complex scalar field $\phi = \Psi/\sqrt{\omega}$. Then the gradient energy is $c^2 \int d^3r |\nabla \phi|^2$, the charge is $Q = (\frac{1}{2}i) \int d^3r (\phi^* \partial_t \phi - \phi \partial_t \phi^*)$, and solutions that we are looking for have the form $\phi(\mathbf{r}, t) = \phi(\mathbf{r}) \exp(i\omega t)$, where the amplitude $\phi(\mathbf{r}) \to 0$ as $r \to \infty$.

The spin-orbit interaction F_D has a very peculiar shape in ^{3}He-B. When $\cos\beta > -\frac{1}{4}$ ($\beta < 104°$), one has

$$F_D = \chi \Omega_L^2 \left[\frac{4\sin^2(\beta_L/2)}{5S} |\Psi|^2 - \frac{\sin^4(\beta_L/2)}{S^2} |\Psi|^4 \right], \tag{5}$$

where β_L is the polar angle of the vector $\mathbf{L}$ of ^{3}He-B orbital angular momentum; and Ω_L is the Leggett frequency, which characterizes the spin-orbit coupling. For $\beta_L = 0$ the spin-orbit interaction becomes identically zero for $\beta < 104°$, while for larger $\beta > 104°$ one has

$$F_D = \frac{8}{15} \chi \Omega_L^2 \left(\frac{|\Psi|^2}{S} - \frac{5}{4} \right)^2, \qquad \cos\beta < -\frac{1}{4}. \tag{6}$$

The form of the Ginzburg-Landau functional in Eq. (6) ensures the formation of the Bose condensate when ω exceeds ω_L. The Bose condensation of magnons is the basis for the HPD: Larmor precession spontaneously acquires a coherent phase throughout the whole sample even in an inhomogeneous external magnetic field. As distinct from the Bose condensates in dilute gases, the formation of HPD starts with the finite magnitude $|\Psi|^2 = (\frac{5}{4})S$, which corresponds to coherent precession with a tipping angle equal to the magic Leggett angle $\beta = 104°$.

For the case, when $\beta_L \neq 0$, the Ginzburg-Landau functional in Eq. (5) includes a positive quadratic term and a negative quartic term, which describes the attractive interaction between magnons. This form does not support the Bose condensation in bulk. However, it is appropriate for the formation of the Q ball in such places in the sample where the potential produced by the $\mathbf{L}$ texture

$$U(\mathbf{r}) = \frac{4\Omega_L^2}{5\omega_L} \sin^2 \frac{\beta_L(\mathbf{r})}{2} \tag{7}$$

has a minimum. The precise form of a Q ball depends on the particular texture and on the position in the container. However, the qualitative behavior of Q balls is generic and can be illustrated using a simple cylindrically symmetric distribution of the $\mathbf{L}$ vector—the so-called flared-out texture realized in the geometry of our experimental cell in the inset of Fig. 1. Far from the horizontal walls and close to the axis of the cell the angle β_L linearly depends on the distance r from the axis: $\beta_L(\mathbf{r}) \approx \kappa r$ (see review [11]). As a result the potential (7) for magnons is $U(r) \propto \kappa^2 r^2$, which corresponds to the harmonic trap used for confinement of dilute Bose gases. The peculiarity of the Ginzburg-Landau functional in Eq. (5) is that the quartic term is not a constant, but is $\propto \kappa^4 r^4$. If the Q ball is formed on the bottom of the cell (see Fig. 1), the initial potential well is three dimensional and can be approximated as $U(r, z) \propto \kappa^2 r^2 z^2/(r^2 + z^2)$.

To find the Q-ball solution, the functional (4) should be minimized with a fixed number of charge Q in Eq. (2). Qualitatively this can done using simple dimensional analysis. Let r_Q and l_Q be the dimensions of the Q ball in radial and in z directions, respectively. For the 2D cylindrical Q ball $l_Q = L$ is the length of the cell, while for the 3D Q ball $l_Q \sim r_Q$. Taking into account that $Q \sim |\Psi|^2 r_Q^2 l_Q$, one obtains the energy (4) of Q ball as function of r_Q and Q:

$$F \sim Q \frac{\Omega_L^2}{\omega_L} \left(\frac{\xi_D^2}{r_Q^2} + \kappa^2 r_Q^2 - \frac{\kappa^4 Q r_Q^2}{S l_Q} \right), \tag{8}$$

where ξ_D is the so-called dipole length characterizing the spin-orbit interaction: in terms of ξ_D magnon mass $m_M \sim \omega_L/(\Omega_L^2 \xi_D^2)$. Minimization of Eq. (8) with respect to r_Q gives the equilibrium radius of the Q ball. While for the 3D Q ball with $l_Q \sim r_Q$ the equilibrium radius exists for any Q, the 2D Q ball is stable only when $Q < SL/\kappa^2$.

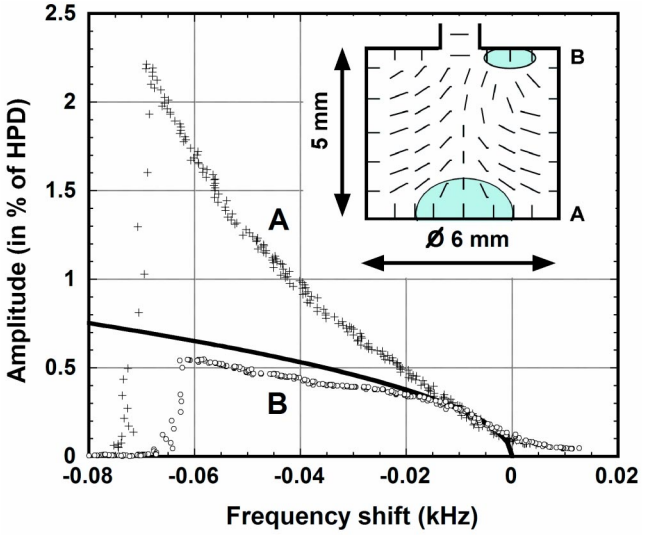

FIG. 1 (color online). The amplitude of persistent signal from the Q balls formed at sites A and B at 1.8 μT excitation, normalized to the full HPD signal. The solid curve is the theoretical estimation in Eq. (13) with $L/\xi_D \sim 10^2$.

In the regime linear in Q (the regime of spin waves) $r_Q \sim \sqrt{\xi_D/\kappa}$ is the characteristic dimension of a spin wave localized in the potential well formed by the flared-out texture. The frequencies of spin-wave modes are

$$\omega_n - \omega_L = a_n \frac{\Omega_L^2}{\omega_L} \kappa \xi_D, \tag{9}$$

where a_n are dimensionless parameters of order unity. In the 2D case these are the equidistant levels of the harmonic oscillator, $a_n \propto (n+1)$, but only even modes $n = 0, 2, 4, \ldots$ are typically excited in NMR experiments [11]. For the 3D case the spectrum is more complicated, since the potential well is not harmonic in general.

In the nonlinear regime, one of the energy levels becomes occupied by magnons. The size of the Q ball grows with Q, and the frequency starts to decrease. This behavior is in agreement with the observation that the persistent signal starts to grow from the linear spin wave localized in the texture [12,13]. During the downward frequency sweep, the spin-wave frequency is trapped by the rf field and after that the amplitude of the signal grows significantly (Fig. 2). This behavior is similar to that of a nonlinear oscillator with small dissipation. For not very large $Q \ll Sl_Q/\kappa^2$, the frequency of the Q ball measured from the frequency of the linear spin wave is

$$\Delta\omega_Q \sim -Q \frac{\Omega_L^2}{\omega_L} \frac{\kappa^3 \xi_D}{S l_Q}. \tag{10}$$

For large Q one must take into account the back reaction of Q to the texture: the Q ball modifies the potential well as can be seen from numerical simulations [14] (Fig. 3).

To compare with the cw NMR experiments, the charge Q must be expressed in terms of the measurable quantity—the total transverse magnetization $M_\perp = \int d^3 r S \sin\beta$ in the persistent signal. For small β one has $M_\perp^2 \sim r_Q^2 l_Q S Q \sim \xi_D l_Q S/\kappa$, which gives the frequency shift of the Q ball as a function of the transverse magnetization:

$$\Delta\omega_Q \sim -\frac{\Omega_L^2}{\omega_L} \frac{\kappa^4 M_\perp^2}{S^2 l_Q^2}. \tag{11}$$

For comparison of the persistent signal with the HPD signal we introduce the total transverse magnetization in the HPD state: $M_{\mathrm{HPD}} \sim SL^3$. Then for the 2D Q ball (with $\kappa^{-1} \sim l_Q \sim L$) and for the 3D Q balls (with $l_Q = r_Q \sim \sqrt{\xi_D/\kappa}$ and $\kappa \sim 1/L$) one obtains

$$\Delta\omega_Q \sim -\frac{\Omega_L^2}{\omega_L} \left(\frac{M_\perp}{M_{\mathrm{HPD}}}\right)^2, \quad \mathrm{2D} \tag{12}$$

$$\Delta\omega_Q \sim -\frac{\Omega_L^2}{\omega_L} \frac{L}{\xi_D} \left(\frac{M_\perp}{M_{\mathrm{HPD}}}\right)^2, \quad \mathrm{3D}. \tag{13}$$

Figure 2 shows the formation of Q balls generated by several spin-wave modes. The signals were recorded at a temperature $T = 0.22 T_c$, pressure 29 bar, and different amplitudes of the rf field (for details, see [12]). By applying different gradients of magnetic field we are able to localize the positions of the Q balls. Signals A and A' correspond to the first and second excited spin-wave modes in the potential well at the bottom of the cell, while the signals B and B' are from the corresponding modes in the potential well at the top of the cell (see inset in Fig. 1). The frequency at which each PS is created corresponds to the frequency of a linear spin wave in Eq. (9). This allows us to estimate $\kappa\xi_D \sim 3.5 \times 10^{-3}$. For $\xi_D \sim 10^{-3}$ cm, the inverse κ is about 1 cm, which is comparable with the dimension of the cell. This demonstrates that the texture that produces the potential wells for magnons A and B is generated by the shape of the sample.

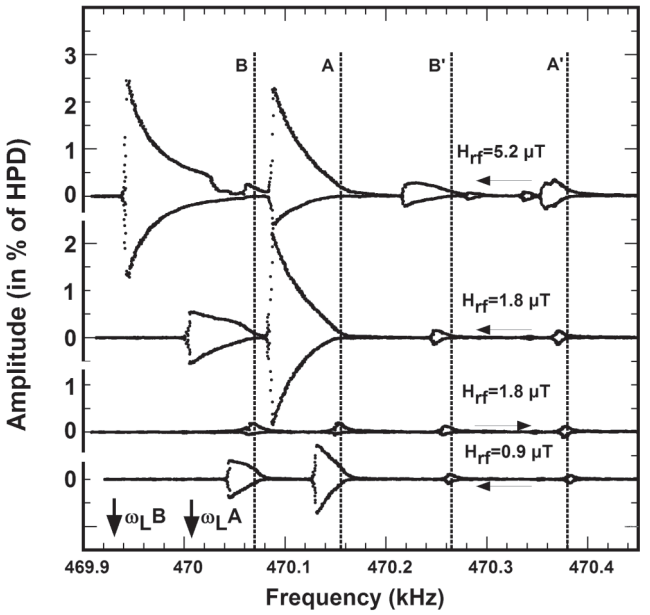

FIG. 2. The cw NMR signals of absorption (negative signals) and full amplitude of deflected magnetization $M_\perp$ (positive signals) in units of full HPD signal, as a function of frequency of the rf field measured for different amplitudes of the rf field H_{rf} and directions of the frequency sweep. The base line is shifted for each signal. Larmor frequency at sites A and B in Fig. 1 is indicated by arrows. At the sweep down, the spin-wave frequency is captured by the rf field and the amplitude of the signal grows.

With the growing Q ball, its frequency decreases approaching the Larmor frequency asymptotically. It is useful to normalize the amplitude of the Q-ball signal to the maximum HPD signal, which corresponds to the case, when all the magnetization inside the cell is homogeneously precessing with the tipping angle $\beta = 104°$. In Fig. 1 the experimental results for the Q balls A and B are compared with the theoretical estimations in Eqs. (12) and (13). The solid line corresponds to Eq. (13) for the 3D Q ball with the fitting parameter $L/\xi_D \sim 10^2$, which is consistent with the dimension L of the cell. In contrast, there is a 2-order-of-magnitude disagreement with Eq. (12) for the 2D Q ball. This demonstrates that at least in the

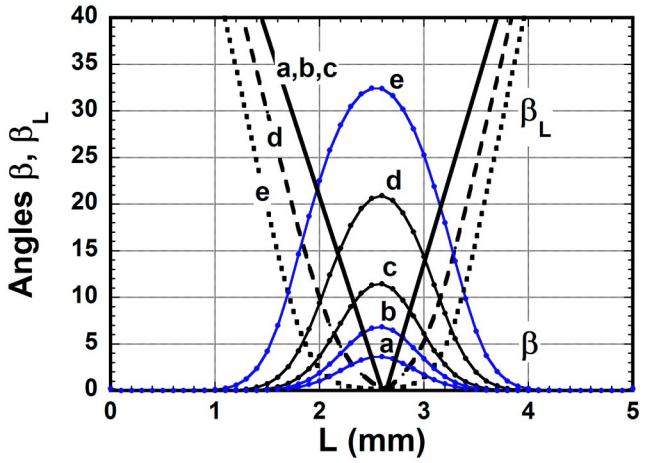

FIG. 3 (color online). Numerical simulation of the Q ball growing in the center of the cell. At small Q, when the β angle of spin $\mathbf{S}$ is less than about 10°, the $\mathbf{L}$ texture is practically Q independent [see $\beta_L(x)$ marked by solid line]. At larger Q the potential well for magnons becomes wider: the dashed line corresponds to the $\mathbf{L}$ texture formed by the Q ball with $\beta = 20°$ in the middle of the Q ball; and the dotted line—with $\beta = 33°$. For details, see [14].

initial stage of Q-ball formation, the Q ball behaves as a 3D object.

At high excitation one can see a large difference between the two Q balls A and B. The more rapid growth of the signal A probably indicates either the development of the 2D Q ball from the 3D one or the effect of self-localization shown in Fig. 3. At high density of magnons condensed into the Q ball, they influence the $\mathbf{L}$ texture so that the potential well becomes wider and can incorporate more magnons. This effect of self-localization is clearly seen in numerical simulations of interacting $\mathbf{L}$ and $\mathbf{S}$ fields (see Fig. 3 for a one-dimensional Q ball). At higher excitation both Q balls lose stability.

We discussed here the Q balls formed in potential wells whose bottom is at $\beta_L = 0$. These are not the only possible Q balls. In the Grenoble experiments [12] the formation of many different Q balls has been observed. They are generated by spin waves in the broad range of frequencies. They can be created, in particular, by topological defects at the walls of the cell.

Q balls can be also formed in pulsed NMR measurements. As distinct from cw NMR, where the Q balls are generated starting continuously from $Q = 0$, in pulsed NMR a Q ball is formed after a large Q is pumped to the cell. In this case the 3D Q ball is often formed on the axis of the flared-out texture, away from the horizontal walls [15]. This clearly demonstrates the effect of self-localization: the main part of the pumped charge relaxes but the rest of Q starts to concentrate at some place on the axis, digging a potential well there and attracting the charge from other places of the container. Moreover, this also shows that Q balls are not necessarily formed at the bottom of the original potential: Q balls may dig the potential well in a different place. Also it is due to the effect of self-localization that the 2D Q ball is unstable toward the 3D Q ball. The Q ball can also be formed with off-resonance excitation [10,14]. In this case the effect of self-localization also plays a crucial role.

In conclusion, the interpretation of an extremely long-lived signal of magnetic induction in ^{3}He-B in terms of Q ball formed by quanta of ϕ field (magnons) is in quantitative agreement with experiments. The Q balls represent a new phase coherent state of Larmor precession. They emerge at low T, when the homogeneous Bose-Einstein condensation of magnons (homogeneously precessing domain) becomes unstable. These Q balls are compact objects which exist due to the conservation of the global $U(1)$ charge (spin projection). At small Q they are stabilized in the potential well, while at large Q the effect of self-localization is observed. In terms of relativistic quantum fields the localization is caused by the peculiar interaction between the charged and neutral fields [16]. The neutral field β_L provides the potential for the charged field ϕ; the charged field modifies locally the neutral field so that the potential well is formed in which the charge Q is condensed.

We are grateful to H. Godfrin and M. Krusius for discussions. This work resulted from collaboration under the ULTI Project (Contract No. RITA-CT-2003-505313) and between the CNRS and the Russian Academy of Science (Project No. 19058), and was supported in part by the ESF COSLAB Programme and by RFBR (Grant No. 06-02-16002-a).

[1] S. R. Coleman, Nucl. Phys. **B262**, 263 (1985).
[2] K. Enqvist and A. Mazumdar, Phys. Rep. **380**, 99 (2003).
[3] A. Kusenko *et al.*, Phys. Rev. Lett. **80**, 3185 (1998).
[4] K. Enqvist and M. Laine, J. Cosmol. Astropart. Phys. 08 (2003) 003.
[5] A. S. Borovik-Romanov *et al.*, JETP Lett. **40**, 1033 (1984); I. A. Fomin, JETP Lett. **40**, 1037 (1984).
[6] G. E. Volovik, arXiv:cond-mat/0701180.
[7] Yu. M. Bunkov, J. Low Temp. Phys. **135**, 337 (2004); *Spin Supercurrent and Novel Properties of NMR in* ^{3}He, edited by W. Halperin, Progress in Low Temperature Physics Vol. 14 (Elsevier, New York, 1995), p. 69.
[8] Yu. M. Bunkov, V. S. L'vov, and G. E. Volovik, JETP Lett. **83**, 530 (2006); **84**, 289 (2006).
[9] Yu. M. Bunkov *et al.*, Phys. Rev. Lett. **69**, 3092 (1992).
[10] D. J. Cousins *et al.*, Phys. Rev. Lett. **82**, 4484 (1999).
[11] M. M. Salomaa and G. E. Volovik, Rev. Mod. Phys. **59**, 533 (1987).
[12] A. S. Chen *et al.*, J. Low Temp. Phys. **110**, 51 (1998).
[13] A. S. Chen *et al.*, J. Low Temp. Phys. **113**, 693 (1998).
[14] Yu. M. Bunkov, J. Low Temp. Phys. **138**, 753 (2005).
[15] D. I. Bradley *et al.*, J. Low Temp. Phys. **134**, 351 (2004).
[16] R. Friedberg *et al.*, Phys. Rev. D **13**, 2739 (1976).